

Ultra-short pulse laser deep drilling of C/SiC composites in air

Chunhui Wang · Litong Zhang · Yongsheng Liu ·
Guanghua Cheng · Qing Zhang · Ke Hua

Received: 10 July 2012 / Accepted: 17 October 2012 / Published online: 31 October 2012
© Springer-Verlag Berlin Heidelberg 2012

Abstract Ultra-short pulse laser machining is an important finishing technology for high hardness materials. In this study, it demonstrated that the ultra-short pulse laser can be used to drill the film cooling holes and square holes in aero-engine turbine blades made of C/SiC composites. Both the edges and bottoms of the drilling holes are covered with small particles. The following factors have a great effect on drilling holes according to this work: (1) circular holes can be processed only at a relative small helical lines spacing. (2) With the increase of laser scanning speed, the depth of holes reduces while the diameter rarely changes. (3) Through the holes of high aspect ratio can be obtained via high processing power.

1 Introduction

In order to ensure aero-engine work safely in a higher temperature, it is a tendency to drill film cooling holes in the aero-engine turbine blades. The film cooling holes can greatly increase the heat transfer coefficient, and the blade experiences a cooler temperature, so that the engine works in a higher flow temperature without affecting the blade [1]. The film cooling holes were traditionally formed by using an

electro-discharge machine (EDM) with a round electrode, which slowly eroded the component materials away until a complete hole was formed. This task is time-consuming and costly for a typical combustion turbine blade requiring hundreds of holes.

C/SiC composites have been identified as the most promising thermal-structural materials for aero-engine applications due to their high thermal stability, high specific modulus, good oxidation, and ablation resistance [2–4]. However, the drilling in blades of C/SiC composites by using EDM is impossible due to the poor conductivity of C/SiC composites. Therefore, it is very promising to drill film cooling holes with high quality and efficiency in blades of C/SiC composites by other ways.

In recent years, the ultra-short pulse laser is extensively used in the field of material processing. For many practical applications, it is a high quality material machining without any visible thermal or mechanical damages at a relative low laser power, and when a high laser power is required, it is similar to long laser pulses ablation. Due to its low thermal diffusion, short laser pulse, and high peak power during laser machining, the ultra-short pulse laser has been widely used in glass, ceramics, plastics, polymers, semiconductors, resin, and other materials of fine machining [5–12]. In addition, the ultra-short pulse laser at high power has been proved to be a practical tool for high-quality deep drilling of metals and 3C-SiC materials [13, 14]. In this paper, the objective is to demonstrate that the ultra-short pulse laser can fabricate holes of C/SiC composites with less than 1 mm in diameter, which own special geometries, superior quality, and high reproducibility. Here, machining circular and square holes with different laser parameters is discussed. The ultra-short pulse laser has the potential to provide a simple fabrication technique that does not require additional post-machining or a special gas environment.

C. Wang · L. Zhang · Y. Liu (✉) · Q. Zhang · K. Hua
Science and Technology on Thermostructure Composite
Materials Laboratory, Northwestern Polytechnical University,
Xi'an, Shaanxi 710072, China
e-mail: yongshengliu@nwpu.edu.cn
Fax: +86-29-88494620

G. Cheng
State Key Laboratory of Transient Optics and Photonics, Xi'an
Institute of Optics and Precision Mechanics, Chinese Academy of
Sciences, Xi'an, Shaanxi 10068, China

2 Experimental

2.1 C/SiC fabrication

T-300TM carbon fiber of about 7 μm in diameter from Toray (Japan) was employed. C/SiC composites, made up of four parts: carbon fibers, PyC interface, SiC matrix, and SiC coating, were processed by using chemical vapor infiltration (CVI) of the SiC matrix into the 2D braid carbon fiber, which performs at ~ 1000 °C. The detailed processing procedures of the C/SiC composites have been described elsewhere [15]. The fiber volume fraction of each performs approximate to 40 %. The density of the C/SiC composites was above 2.0 g/cm^3 and the porosity was 10–20 %. The size of specimen of C/SiC composites was 20 mm \times 10 mm \times 3 mm. Before being machined, the specimens were cleaned with alcohol in an ultrasonic bath for 15 min.

2.2 Machining experiment

The ultra-short pulse laser systems machining samples belong to State Key Laboratory of Transient Optics and Photonics, Xi'an Institute of Optics and Precision Mechanics, Chinese Academy of Sciences. It is controlled by a computer, where the laser, the positioning system and the scanner are operated simultaneously. The machining process was carried out in the atmosphere of air under the temperature of 20–26 °C with the room humidity of 40–50 %. The specimens were placed on a motorized XYZ translation stage, which was used to pattern square and circular holes, even more complex geometries. The laser beams were perpendicular to the surfaces of specimens and the machining was considered completed when the holes' depth did not change with the increase of laser pulses.

The circular holes in this experiment can be divided into two kinds: blind ones and through ones. Trepanning and helical drilling, usually collectively called trepanning, is a combination of percussion drilling and laser beam movement relative to the target. In the experiments, two different processing laser systems were selected. The laser system, which generates 1 ps laser pulses with the laser wavelength at 1030 nm and at a 100 kHz repetition rate with a processing focal length at 80 mm, is used for drilling blind holes of a relatively large taper with about 600 μm in diameter. In order to get through holes of low time consuming and high aspect ratio, another laser system is utilized at 532 nm. The maximum laser power is 20 W with the pulse width at about 10 ps. For the laser beam focusing, a lens with a focal length of 100 mm is used in the processing.

Square holes were carried out at an import-integrated laser micromachining system that the maximum repetition rate, center wavelength, and pulse width were 1 kHz, 800 nm

and 80 fs, respectively. The laser was adjusted to focus on the C/SiC composites specimens to machine it layer by layer until a square hole was produced. A 5X objective lens with NA = 0.14 nm and the focal length at 100 mm were used in the processing.

2.3 Sample characterization

The machining morphology features of C/SiC composites were examined by a scanning electron microscope (SEM). Energy dispersive spectroscopy (EDS) was used to identify the elemental composition transformation between the untreated and laser-treated area.

3 Results and discussion

3.1 The circular holes

Under the initial parameters of the helical lines spacing at 0.2 mm with a 1000 mm/s scanning speed, a circular hole try to be drilled, but only get a donut shape, which is similar to Fig. 1. Then the helical lines spacing was reduced to 0.05 mm by adjusting the beam trajectory relative to the sample, and ultimately get a blind taper hole as shown in Fig. 2.

Figures 1(a) and 2(a) show a donut shape and blind circular hole with the scanning speed at 1000 mm/s before any debris removed, respectively. There are a number of particles on the bottom, the walls, and around the cavity and EDS indicates that the particles are composed of C, Si, and O. Some of the particles can be easily removed by plain washing and scrubbing, showing a loose adhesion. And the others, to the contrary, show a relative high adhesion. Figures 1(b) and 2(b) show the donut shape and the circular hole after cleaning 30 min in an ultrasonic bath with alcohol. After cleaning, helical traces can be seen clearly in the donut shape. The blind circular hole has a nearly circular shape with diameter about 600 μm . Because of the Gaussian distribution of the laser pulses, a certain degree of taper was found in the machined hole. In conclusion, the SEM images show a small heat-affected area of thermal damage.

Maybe the question still not answered is why under the conditions with other same parameters, there is a certain depth blind hole with the helical lines spacing at 0.05 mm while helical lines spacing at 0.2 mm can only get a light donut shape. The concept of fluence threshold for ablation was used to explain this phenomenon [16–19]. The laser machining completed at maximum depth for the attenuation of pulse fluence to the ablation threshold in the drilling processing. In other words, there will be no large change of the holes with more number of laser pulses. Since the machining is generally achieved by a large number of consecutive

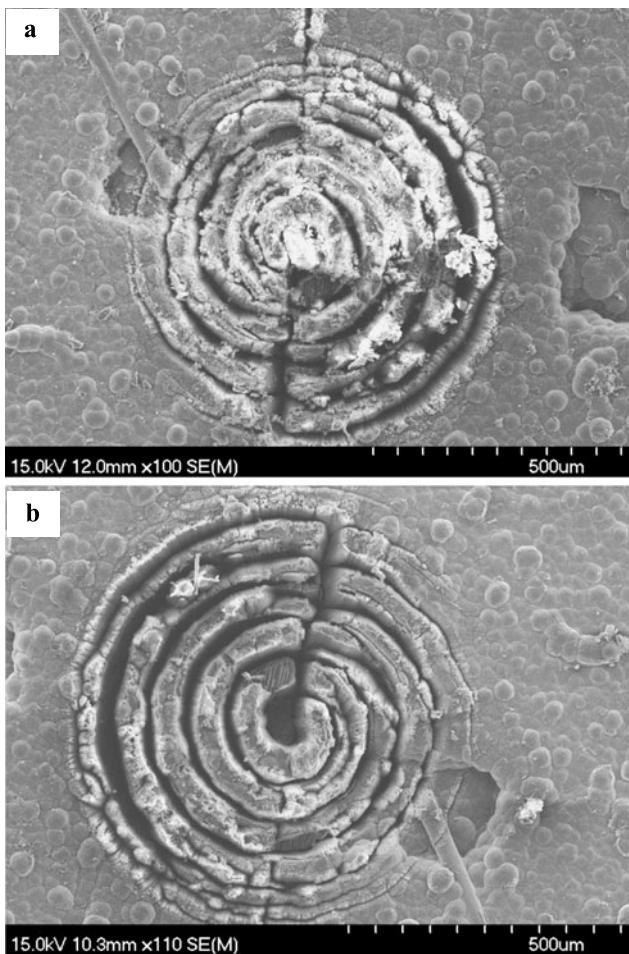


Fig. 1 SEM images of a donut shape drilled with helical lines spacing at 0.2 mm and scanning speed at 1000 mm/s in air: (a) before cleaning, (b) after cleaning 30 min in an ultrasonic bath with alcohol

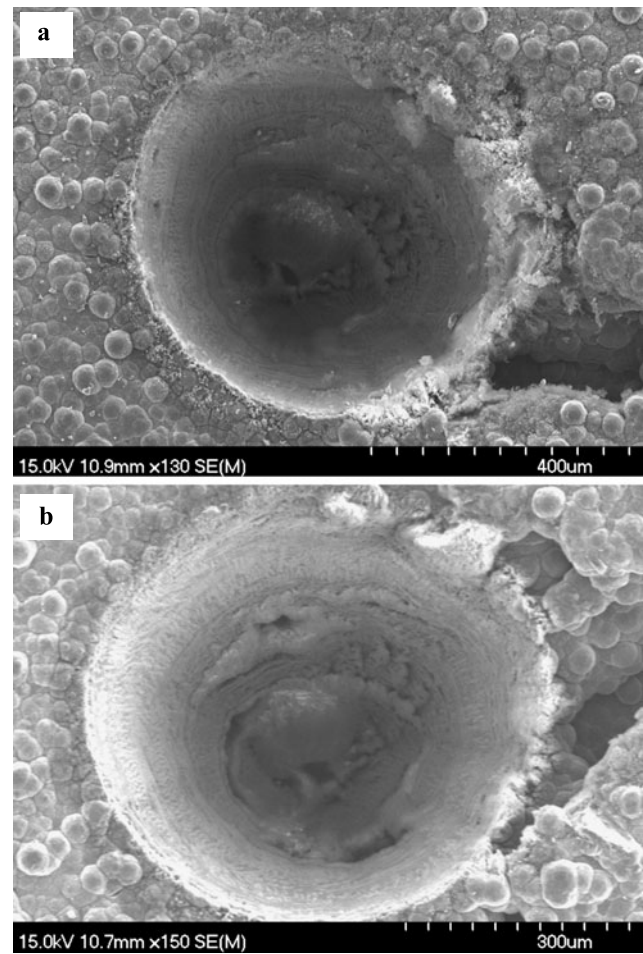


Fig. 2 SEM images of a blind circular hole with helical lines spacing at 0.05 mm and scanning speed at 1000 mm/s in air: (a) before cleaning, (b) after cleaning 30 min in an ultrasonic bath with alcohol

pulses, each pulse is first guided through the channel formed by the previous pulses, and it is absorbed by C/SiC composites at the end of the channel, making its own contribution to machining.

In order to understand the physics involved in the machining process, it demonstrates the results on the dependencies between the diameters and depths of circular holes fabricated in air after cleaning and the laser scanning speed. Figure 3 shows the changes of different specimens after machining with the laser scanning speed at 100, 500, 1000, 1500, and 2000 mm/s, respectively. The depth of holes reduces while the diameter has little change with the laser scanning speed increasing. The effects is not surprising for processing blind holes in air and the same result is also demonstrated in another literature [20]. With the increase of laser scanning speed, there is less time to escape from drilled blind holes for debris and particles produced by the ultra-short pulse laser. The debris and particles of the blind holes' bottom are difficult to escape from the holes while the debris of the entrance edge spreads out easily. More debris

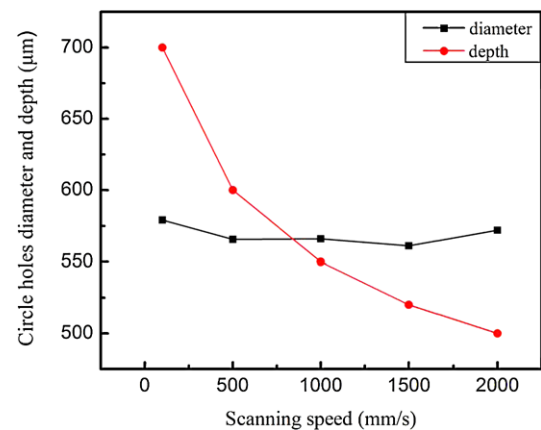


Fig. 3 Dependencies of the diameters and depths of the circular holes fabricated after cleaning on the laser scanning speed

and particles inside the blind holes reduce the threshold for optical break down of air and plasma formation, and then produce a bigger plasma volume and stronger plasma ma-

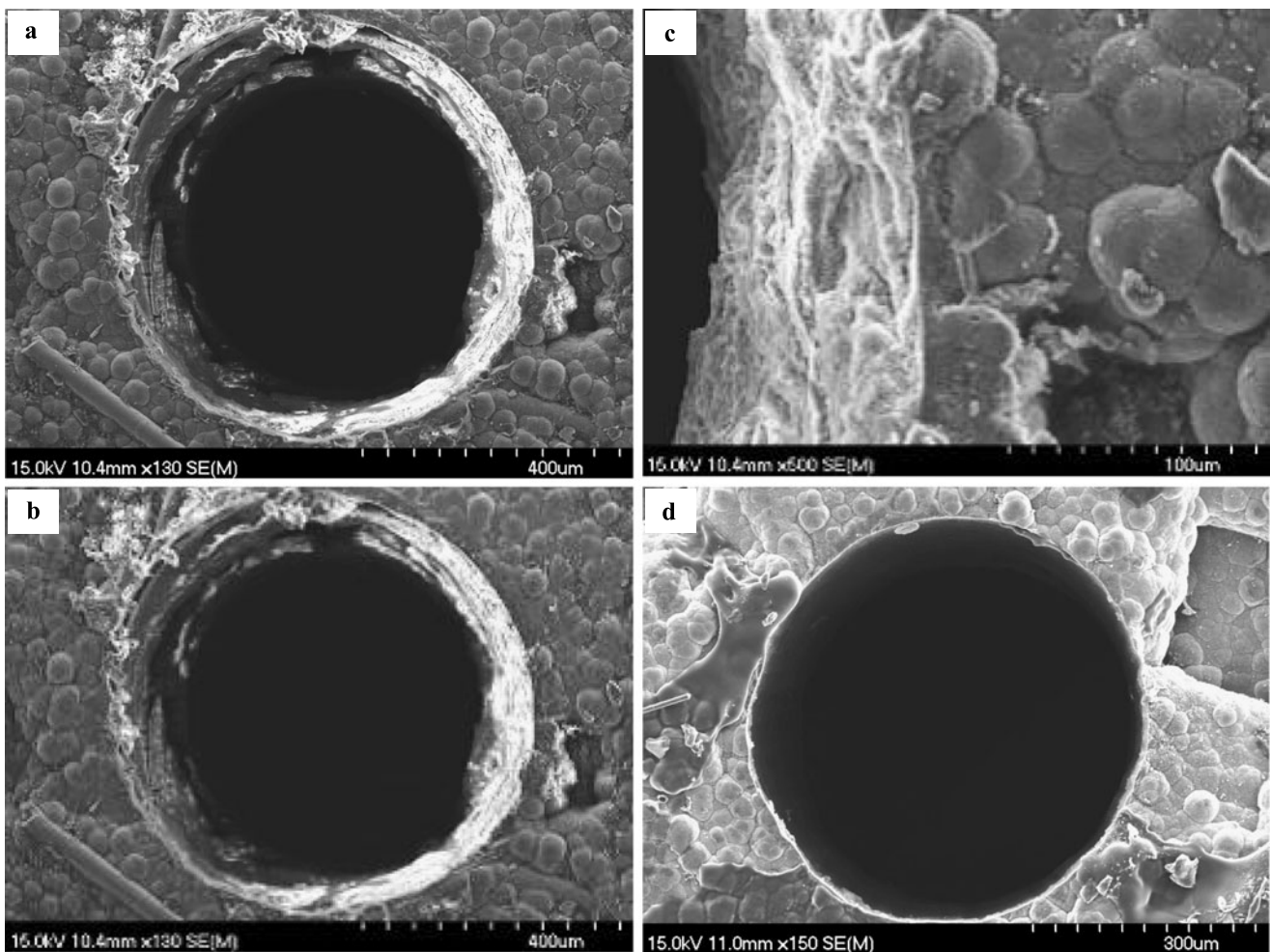


Fig. 4 SEM images of a circular hole drilled in air: (a) the top side of the drilling circular hole before cleaning, (b) the top side of the drilling circular hole after cleaning, (c) at the edge of hole of (b), (d) the bottom of the drilling circular hole before cleaning

chining of the blind holes. Therefore, these lead to decreasing of the blind holes' depth with the increase of scanning speed. These effects are not relevant for the entrance edge, where debris and particles can freely move and escape from the holes in the laser pulses interval time. So, there is no fundamental change of the diameter in machined holes with the scanning speed increasing.

In order to get a through hole of good quality, low time consuming, and high aspect ratio, the hole was drilled with three times: it is the first processing parameters of processing power at 19.5 W and repetition frequency at 400 kHz; it is the second processing parameters of processing power at 17.5 W and repetition frequency at 400 kHz; and it is the finally processing parameters of processing power at 311 mW and repetition frequency at 32 kHz.

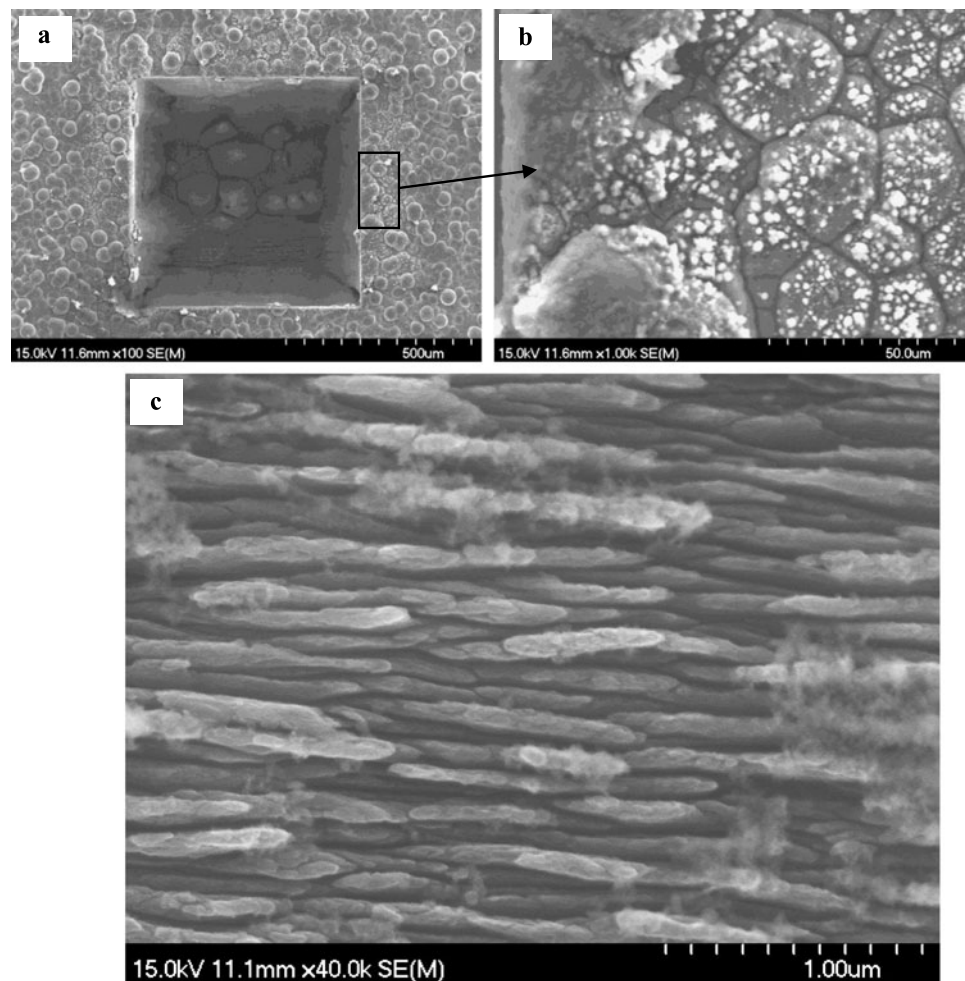
Figure 4 SEM micrographs show a circular hole of C/SiC composites. Figure 4(a) shows one of the drilling holes before any debris removal was carried out, and the particle size of which was about 50 nm–1 μ m. Figure 4(b) shows the

top side of the hole after scrubbing and cleaning in an ultrasonic bath with alcohol for 30 min. This debris can be very hardly removed by plain washing and scrubbing and there is a tight arrangement of large debris and small particles around the cavity. The surrounding area has apparent circular cutting traces, oxide layers, and visible heat-affected areas (Fig. 4(c)). In general, the SEM images show that the thermal damage becomes small at the bottom (Fig. 4(d)). It has a nearly circular shape. The bottom side of the hole displays very small surrounding debris and is shown in this photograph (Fig. 4(d)) without any prior cleaning. In addition, the machining processing rules and optimizations of through holes will be introduced in the future work.

3.2 The square holes

The morphological changes of a square hole after machining with the ultra-short pulse laser in C/SiC composites are depicted in Fig. 5(a). Both the edge and bottom are covered with small particles. Otherwise, some particles have

Fig. 5 The ultra-short pulse laser machining the square hole on C/SiC composites after cleaning: **(a)** square hole; **(b)** at the edge of **(a)**; **(c)** magnification of the part of bottom in the SEM image of **(a)**, showing waviness



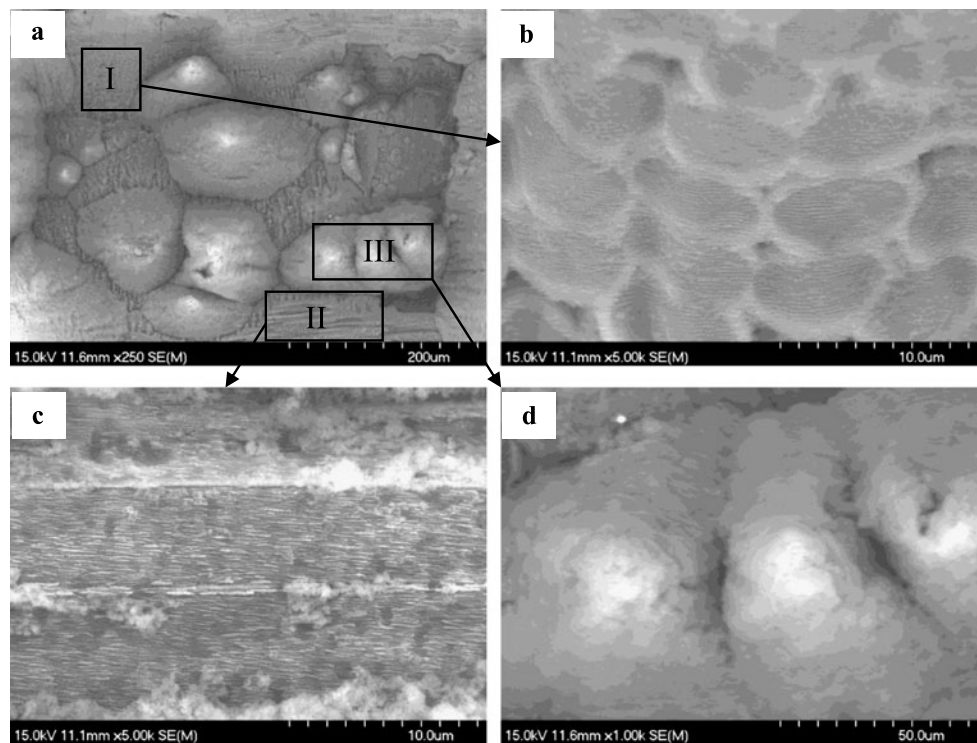
been deposited next to the cavity (Fig. 5(b)). Waviness features can be observed in a magnified SEM micrograph in the part of the bottom and wall (Fig. 5(c)). These waviness features are generally described as ripples or laser induced periodic surface structures for other materials [21–25]. EDS indicated that the particles were composed of C, O, and Si.

Figure 6 shows SEM micrographs of the bottom in Fig. 5(a). Figure 6(a) shows SEM micrograph of the bottom region. Clearly, there are three zones in this region, the zone I where the fibers were perpendicular to the bulk surface, the zone II where the fibers were parallel to the surface and the zone III showing the SiC matrix and PyC interfacial layer. Figure 6(b) shows that there is no melt phase and the carbon fiber cross-section displays features of the brittle fracture. Furthermore, the periodic structures paralleling to the fracture surface-occurred with width of 150–250 nm, which can be called ripples were generated as well. Formation of the ripples is believed to result from the nonuniform surface energy distribution [26, 27]. Figure 6(d) shows that cone-like submicron waviness structures also can be observed on the carbon fiber fracture surface, which is perpendicular to the carbon fiber surface. Obviously, the parti-

cles are not evenly distributed on the sample surface from Figs. 6(b) and (d). There are more particles on sedimentary areas of the adjacent fiber gaps. From the zone III (see Fig. 6(c)), layered cone-shaped cell body with parts of SiC particles were formed at thermal oxidizing atmosphere. The mismatch of the thermal expansion coefficients between the fibers and SiC matrix may be one of the most important reasons for determining a clearly different morphology of the bottom.

Can be clearly seen that the ablation of zone III is serious than the zone I and II, which is due to the competition of the two processes, electron–phonon coupling and diffusion to a lower temperature region. This is determined by the parameter of electron–phonon coupling coefficient, g . For a larger g , electrons can transfer more energy locally to the adjacent lattice and the thermalization between electrons and lattice will reach sooner. Whereas, for a small g , electron diffusion should play a dominate role. It is difficult for electrons transferring energy to adjacent lattice and the temperature of the electronic system and the lattice system is very uneven. Therefore, the electron–phonon coupling coef-

Fig. 6 SEM micrograph of the square holes machining of the bottom C/SiC composites: (a) in the bottom; (b) zone I in (a); (c) zone II in (a); (d) zone III in (a)



efficient is larger, the more uneven of thermal spatial distribution and more powerful ablation [28].

4 Conclusions

- (1) A circular hole can be obtained when choosing a relatively small helical lines spacing, otherwise, a donut shape can only be obtained. As the laser scanning speed increases, the depth of holes reduces and the diameter has little change. The edge and bottom of the circular and square holes are all covered with small particles. Due to the heterogeneity of the composites, the bottom of machining square holes shows a clearly different morphology of cone-shaped cell and waviness.
- (2) Ultrashort pulse laser machining has been demonstrated as a practical tool for the high-quality, angled, and deep drilling holes in C/SiC composites. Explanations supporting the advantages of the ultra-short pulse laser have been given. However, some important questions are still left for the future: Whether we can change the processing parameters to improve the quality of the laser through holes? Can the ultra-short pulse laser do this job at the same speed or faster? We are quite confident that one will soon be able to give affirmative answers to these questions.

Acknowledgements The authors acknowledge the support of the major national scientific instrument and equipment development

project (2011YQ12007504), the Research Fund of State Key Laboratory of Transient Optics and Photonics (No. 201106), the Northwestern Polytechnical University (No. 20120204), the Chinese National Foundation for Natural Sciences under Contracts (Nos. 51002120, 51032006), and the “111” project (No. 08040).

References

1. D. Jorge, R. Luis, *J. Mater. Process. Technol.* **143–144**, 342 (2003)
2. R. Naslain, *Compos. Sci. Technol.* **64**, 155 (2004)
3. M. Rosso, *J. Mater. Process. Technol.* **175**, 364 (2006)
4. L.T. Zhang, L.F. Cheng, Y.D. Xu, *Aeronaut. Manuf. Technol.* **1**, 24 (2003)
5. P.P. Pronko, S.K. Dutta, J. Squier, J.V. Rudd, D. Du, G. Mourou, *Opt. Commun.* **114**, 106 (1995)
6. C. Momma, B.N. Chichkov, S. Nolte, F. von Alvensleben, A. Tünnermann, H. Welling, *Opt. Commun.* **129**, 134 (1996)
7. B.N. Chichkov, C. Momma, S. Nolte, F. von Alvensleben, A. Tünnermann, *Appl. Phys. A* **63**, 109 (1996)
8. B.C. Stuart, M.D. Feit, S. Herman, A.M. Rubenchik, B.W. Shore, M.D. Perry, *J. Opt. Soc. Am. B* **13**, 459 (1996)
9. P. Simon, J. Ihlemann, *Appl. Phys. A* **63**, 505 (1996)
10. W. Kautek, J. Krüger, M. Lenzner, S. Sartania, C. Spielmann, F. Krausz, *Appl. Phys. Lett.* **69**, 3146 (1996)
11. H. Varel, D. Ashkenasi, A. Rosenfeld, M. Wähmer, E.E.B. Campbell, *Appl. Phys. A* **65**, 367 (1997)
12. S. Nolte, C. Momma, H. Jacobs, A. Tünnermann, B.N. Chichkov, B. Wellegehausen, H. Welling, *J. Opt. Soc. Am. B* **14**, 2716 (1997)
13. G. Kamlage, T. Bauer, A. Ostendorf, B.N. Chichkov, *Appl. Phys. A* **77**, 307 (2003)
14. M. Farsari, G. Filippidis, S. Zoppel, G.A. Reider, C. Fotakis, J. Micromech. Microeng. **15**, 1786 (2005)

15. H. Mei, L.F. Cheng, L.T. Zhang et al., *Carbon* **44**, 121 (2006)
16. J. Psikal, V.T. Tikhonchuk, J. Limpouch, A.A. Andreev, A.V. Brantov, *Phys. Plasmas* **15**, 053102 (2008)
17. O. Klimo, J. Psikal, J. Limpouch, J. Proška, F. Novotny, T. Cecchetti, V. Floquet, S. Kawata, *New J. Phys.* **13**, 053028 (2011)
18. A. Picciotto, D. Margarone, J. Krasa, A. Velyhan, E. Serra, P. Bellutti, G. Scarduelli, L. Calliari, E. Krousky, B. Rus, M. Dapor, *Europhys. Lett.* **92**, 34008 (2010)
19. A. Picciotto, D. Margarone, M. Crivellari, P. Bellutti, S. Colpo, L. Torrisi, J. Krasa, A. Velhyan, J. Ullschmied, *Appl. Phys. Express* **4**, 126401 (2011)
20. T. Jiang, Q.L. Zhao, Z.W. Dong, R.W. Pan, X. Yu, *Infrared Laser Eng.* **39**, 1044 (2010)
21. J. Bonsea, A. Rosenfeldb, J. Krügera, *Appl. Surf. Sci.* **257**, 5420 (2011)
22. O. Varlamova, F. Costache, M. Ratzke, J. Reif, *Appl. Surf. Sci.* **253**, 7932 (2007)
23. J.P. Colombier, E. Audouard, P. Combis, A. Rosenfeld, I.V. Hertel, R. Stoian, *Appl. Surf. Sci.* **255**, 9597 (2009)
24. S. Juodkazis, K. Nishimura, H. Misawa, *Appl. Surf. Sci.* **253**, 6539 (2007)
25. J. Vincenc Obonaa, V. Ocelíka, J.Z.P. Skolski, V.S. Mitko, G.R.B.E. Römerc, A.J. Huis in't Veld, J.T.M. De Hossona, *Appl. Surf. Sci.* **258**, 1555 (2011)
26. D.J. Ehrlich, S.R.J. Brueck, J.Y. Tsao, *Appl. Phys. Lett.* **41**, 630 (1982)
27. J.C. Wang, C.L. Guo, *Appl. Phys. Lett.* **87**, 251914 (2005)
28. Y. Dong, P. Molian, *Appl. Phys. A* **77**, 839 (2003)